ORIGINAL PAPER

Colorimetric-enzymatic determination of tyramine by generation of gold nanoparticles

Jesús Navarro[1] · Susana de Marcos[1] · Javier Galbán[1]

Abstract

In this paper, it has been demonstrated that Au(III) is able to act instead of O_2 in the oxidase enzymatic reaction, so that it becomes reduced to purple gold nanoparticles (AuNPs). The plasmon band (at 540 nm) can be used as the analytical signal. Tyramine has been determined using its enzymatic reaction with tyramine oxidase (TAO). The kinetic of the AuNP formation has been studied in the light of both the Avrami equation for crystallization and the Finke-Watsy mechanism for AuNP nucleation and growth. The effects of the Au(III), TAO and tyramine concentrations on the corresponding kinetic constants have been investigated. Working at room temperature, under optimal conditions (phosphate buffer pH 7.0, TAO 0.5 U.mL^{-1} Au(III) 1 mM), the linear response ranges from 2.5×10^{-5} M to 3.3×10^{-4} M Tyramine (5.6% RSD) and the LOD is 2.9×10^{-6} M. Under these conditions, the signal is measured after 30 min reaction (to obtain the highest sensitivity), but this time can be significantly reduced by increasing the temperature (the reaction is finished after 4 min when working at 50 °C). The method has been applied to tyramine determination in a cheese sample with good results. The new scheme proposed in this paper can be extended, in principle, to other enzymatic methods based on oxidase enzymes.

Keywords Tyramine · Tyramine oxidase · HRP · ABTS · TMB · Foodstuff

Introduction

Tyramine is a biogenic amine produced by the decarboxylation of the aminoacid tyrosine due to biological activity (microorganisms). It is usually present in foodstuffs in moderate concentrations. High concentrations in foodstuffs of this compound, which can appear due to inadequate manipulation or decomposition, are not suitable for human consumption (its toxic effects include nausea, vomiting, migraines or respiratory disorders) [1]. The tyramine contents in foods is not specifically regulated by law although it is strongly suspected that it helps the histamine concentrations in the human body to increase (the concentration limits of histamine in some foods have been established by the European Union). Moreover, tyramine is the majority biogenic amine in some types of foods and its maximum content in some products is regulated in the corresponding Codex Alimentarius of some countries [2].

The determination of tyramine in foods presents similar difficulties to the analysis of other biological substances: the complexity of the sample matrix and its low concentration. This is why it is almost unavoidable to perform a previous extraction to eliminate the interferences, to concentrate the samples and to apply an instrumental separation technique such as layer chromatography, gas chromatography, capillary electrophoresis or high-resolution liquid chromatography. These methodologies have been described in previous papers [3, 4]. All these methods work very well, but they need long analysis time and qualified personnel, so they are normally used when several biogenic amines need to be determined. Rapid response methods are necessary for the rapid detection of high levels of tyramine in foods in order to adequately protect consumers, workers and producers. Enzymatic methods of analysis are suitable alternatives in these cases.

✉ Javier Galbán
jgalban@unizar.es

[1] Analytical Chemistry Department, Faculty of Sciences, Aragón Institute of Nanoscience (INA-ICMA), University of Zaragoza, E-50009 Zaragoza, Spain

Very few enzymatic reactions work analytically well for tyramine, in particular, those based on Polyamine Oxidase (PAO) and especially Tyramine Oxidase (TAO) [5]. TAO is an oxidase enzyme which catalyzes the oxidation/decarboxylation of tyramine according to the reaction given in Scheme 1. TAO has been used for the development of electrochemical sensors [6, 7], but as far as we know, no optical colorimetric or fluorometric methods or sensors have been developed for the determination of this compound.

The current strategies used for colorimetric determinations based on oxidase reactions, such as that shown in Scheme 1, consist of coupling an indicating reaction based on horseradish peroxidase (HRP) and a chromogen (TMB, ABTS, or some others) which is oxidized to a colored form (the reduced form is colorless).These reactions generally work well but present some problems [8, 9]: a) most dyes are not very stable and can be partially oxidized by the O_2 present in the air; b) the colored species formed can react with the product of the analyte; c) several reducer species present in the sample can interfere in the dye product formation. New strategies to avoid these problems are required.

The use of AuNPs as a basis for the development of colorimetric methods has been growing exponentially. Most of these methods are based on using the AuNPs as a substitute for the chromogenic reagent and exploit three fundamental ideas [10, 11]: 1) The addition of the analyte causes the aggregation of these nanoparticles so that they change their spectroscopic properties in a way related to the analyte concentration in the sample, 2) as a consequence of the enzymatic reaction the AuNPs size increases due to the H_2O_2 presence [12]; and 3) The product of the enzymatic is able to form AuNPs [13].

In this paper we propose a different approach which complements these AuNPs methods and solves some of the previously indicated problems caused by chromogens. It consists of synthesizing AuNPs from Au(III) as a consequence of the enzymatic reaction and measuring the absorbance of the appearing plasmon band (540 nm).
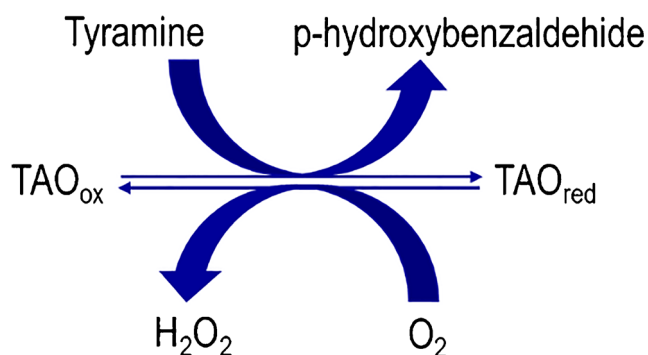
Our hypothesis is that Au(III) can replace O_2 in the reaction of Scheme 1, so it is reduced and AuNPs appear during the enzymatic reaction. Taking advantage of the good selectivity of TAO to tyramine, interference problems are minimized. This has allowed this method to be applied for tyramine determination in a cheese sample. Experimental conditions have been obtained in which the formation of nanoparticles occurs in a few minutes. This method complements one of the three ways in Analytical Nanoscience proposed by Valcarcel [14].

Experimental section

Reagents and solutions

Tyramine oxidase (TAO) (EC 1.4.3.6) was obtained from Sekisui Diagnosis (https://www.sekisuichemical.com) (4. 6 U.mg^{-1}) and dissolved in phosphate buffer pH 7.0, 0.1 M. The biogenic amines tyramine, cadaverine, putrescine and histamine were obtained from Sigma (https://www.sigmaaldrich.com/spain.html); these amines were weighed and dissolved in the corresponding buffer. Phosphate buffer (0.1 M) was prepared from Na_2HPO_4 and NaH_2PO_4 solids (Sigma S9763, S9638). Gold(III) chloride hydrate solid (Sigma 254,169) was dissolved in miliQ water to obtain a 50 mM solution.

Apparatus

A Foxy-RTM fluorescence O_2 sensor from Ocean Optics (EW Duive, The Netherlands, https://oceanoptics.com/) consisting of a QE65000 CCD-array spectrometer coupled to an oxygen FOXY-R (by A QBIF600-UV/Vis optical fiber), and a LS-450 pulsed blue LED light as radiation source, was used to measure dissolved oxygen. A Tecnai F30H–7650 microscope (scanning and transmission mode, STEM) (FEI, The Netherlands, https:// www.fei.com) was used for characterization of the gold nanoparticles. UV-vis molecular absorption measurements were performed on a Specord 210 Plus spectrophotometer and an Agilent 8453 diode array spectrophotometer (One cm cuvettes were used in all cases). A Thermo Scientific Multifuge X1R centrifuge was used for separation by centrifugation. The Millipore MiliQ H_2O system was used for water purification.

Sample treatment

Ten grams of Emmental cheese were weighed and mechanically ground with 20 mL of trichloroacetic acid (TCA) 5% (w/V). The mixture was stirred for 30 min and subsequently

Scheme 1 Enzymatic oxidation of tyramine catalyzed by Tyramine Oxidase (subscript "ox" and "red" refer to oxidized and reduced forms of TAO, respectively)

centrifuged for 20 min at 5000 rpm at 4 °C. The supernatant was collected and 2 mL of 2 M NaOH was added and centrifuged again for 20 min at 5000 rpm at 4 °C. The supernatant was collected and the pH was adjusted to pH 7.0 with HCl 1 M. The extract was filtered with a 0.45 μm nylon filter and the solution was made up to 25 mL with miliQ H_2O. This sample solution was used for the determination of tyramine in cheese.

Measurement procedure

1940 μL of the corresponding standard solution (in phosphate buffer pH = 7.0 0.1 M) and 20 μL TAO 0.5 U.mL^{-1} were added in a cuvette. After waiting 5 min, 40 μL of 50 mM HAuCl$_4$ were added to the cuvette. The formation of AuNPs was followed by measuring the variation of Abs (540 nm) with time at room temperature and at 40 °C. To perform the kinetic study, spectra were collected every 5 s after adding the HAuCl$_4$ solution.

For the determination of tyramine in Emmental cheese, 250 μL of the sample solution, 1690 μL phosphate buffer pH = 7.0 0.1 M and 20 μL TAO 0.5 U.mL^{-1} were added in a cuvette. After waiting 5 min, 40 μL of 50 mM HAuCl$_4$ were added to the cuvette and the formation of AuNPs was followed.

Results and discussion

Mechanism of the enzymatic reaction in the presence of au(III)

The molecular absorption spectra of a solution containing tyramine, TAO and Au(III) change during the enzymatic reaction, as shown in Fig. 1a. As can be seen, after an activation time, a band due to the plasmon resonance appears and increases until a plateau is obtained (Fig. 1b). Depending on the experimental conditions used, a later slower increase is observed. Figure S1 (Supporting Information) shows TEM images indicating that the spectra are due to the AuNP formation.

Several hypotheses were considered in order to explain the AuNP formation, before establishing the final mechanism:

i) Intrinsic reducing capabilities of proteins: Some proteins are able to generate Au nanostructures due to the reducing capability of some aminoacids [15]; however, in this case, no AuNP formation was observed by direct reaction between Au(III) and TAO (Figure S2A).

ii) Intrinsic reducing capabilities of tyramine: Previous papers have shown that AuNP can be formed by direct reaction between nitrogenated compounds and Au(III) [16]. The direct reaction between tyramine and Au(III) was thoroughly studied but no AuNP formation was
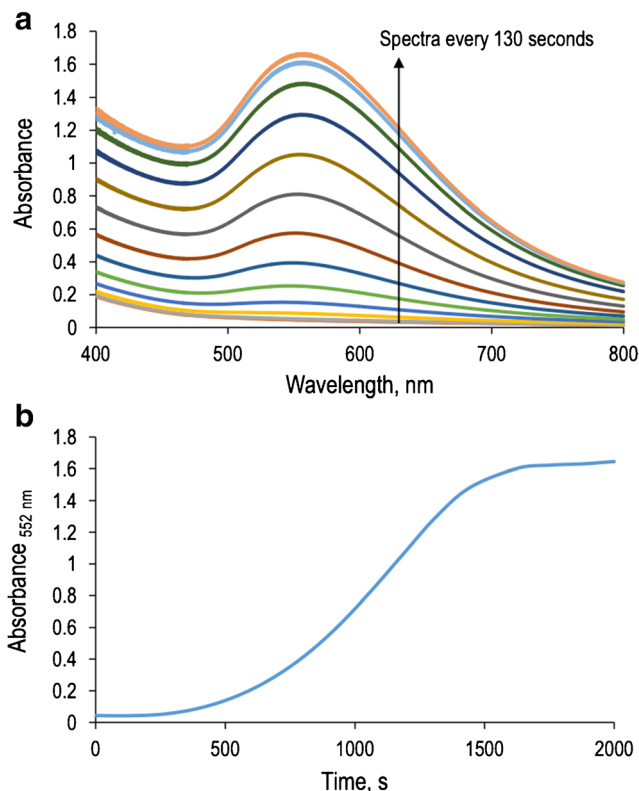

Fig. 1 Molecular abosortion spectra of gold nanoparticles (AuNP) formation during the enzymatic reaction. Experimental conditions: [TAO] = 0.5 U.mL^{-1}, [Au(III)] = 1 mM, [tyramine] = 2.6×10^{-4} M, incubation time 5 min and pH 7.0 phosphate buffer 0.1 M, at room temperature (Fig. **b** shows the absorbance at the maximum wavelength)

observed. It is only when using a large amount of tyramine that a black Au^0 precipitate appears after several hours of reaction, giving a small signal (Figure S2B). This study was also carried out in the presence of albumin but no changes were observed (Figure S2C).

iii) AuNP growth induced by H_2O_2: Several authors have indicated that H_2O_2 is able to increase the growth of previously formed AuNP [12, 17]. Thus, the Au^0 nucleus can be formed by direct reduction of Au(III) with tyramine, where H_2O_2 assists the AuNP growth. To test this, the enzymatic reaction was carried out in the presence of catalase (Figure S3) to remove the H_2O_2 formed during the enzymatic reaction. The catalase produced rather the opposite effect, increasing the kinetic of AuNP formation and reducing the width of the spectra. Moreover, catalase increases the rate of the AuNP formation, which indicates that H_2O_2 actually hinders the process.

iv) Au(III) versus O_2: Finally, as shown below, the kinetic of the AuNP formation increases when the tyramine concentration is higher than that of the O_2 (i.e. the whole O_2 of the solution is consumed), indicating that the Au(III) participates in the enzymatic reaction. The possibility that metallic ions can act as substrates of enzymes has recently been reported [18].

All these studies reinforce the idea that the active center of the enzyme is responsible for the AuNP. According to this, Au(III) is reduced to gold nanoparticles and the catalytic center of the enzyme is oxidized to its initial state. TAO is an enzyme belonging to the copper-containing amine oxidases group. The kinetic mechanism of this type of enzyme has been studied [19] (not specifically with TAO) and is summarized in figure S4. As can be seen, during the reaction Cu(II) can be reduced to Cu(I) and it is reoxidized back by O_2. Since Cu(I) is also able to reduce Au(III) to Au^0, this can demonstrate the proposed mechanism.

Kinetics of the AuNP formation: theoretical background

In this paper we are interested in providing theoretical support and understanding of the experimental results obtained. Most of the classical mechanisms [20, 21] consider that the formation of nanoparticles is based on the Johnson, Mehl, Avrami and Kolmogorov (JMAK) crystallization model which is given by the general equation:

$$\frac{Abs_t}{Abs_\infty} = 1 - e^{-(kt)^n} ==> Ln\left(Ln\left(\frac{Abs_\infty}{Abs_\infty - Abs_t}\right)\right)$$
$$= nLn(K_{Av}) + nLn(t) \tag{1}$$

Abs_t and Abs_∞ being the absorbance of the plasmon band at any moment and at the end of the reaction respectively, K_{Av} being the overall kinetic constant (Avrami constant) of the AuNP formation reaction and n being a parameter related to the dimensionality and shape of the AuNPs. During the optimization study, the $Abs_t = f(t)$ representations were fitted to this equation and the corresponding K values were obtained.

Starting with these principles, Finke-Watzy proposed a kinetic mechanism consisting of two simultaneous steps [22], the first being a slow continuous pseudo-first order reaction describing the formation of nuclei involving the precursor (Au(III) in this case) (Eq. 2), and a second fast step (Eq. 3) comprising an autocatalytic growth of the nuclei with the precursor,

$$A \Rightarrow^{k_1} B \tag{2}$$

$$B + A \Rightarrow^{k_2} 2B \tag{3}$$

They derived an equation relating the $[A]_t$ concentration with k_1, k_2 and $C_{A,0}$ (initial A concentration):

$$[A]_t = \frac{k_1 + k_2 C_{A,0}}{k_2 C_{A,0} + k_1 e^{(k_1 + k_2 C_{A,0})t}} \tag{4}$$

From this equation, both $[B]_t$ and $[AuNP]_t$ can be derived. Although other models have been subsequently proposed, the Finke-Watsy mechanism has been extensively used for

modeling gold or other nanoparticle formation (and other types of structures, such as protein agglomeration) [23]. In most cases, the reducer concentration (necessary for Au^0 formation) is in excess of A, so k_1 and k_2 are pseudo-first and second order constants, respectively. In our case the reducer is not always in excess relative to Au(III), but in most cases it is in defect so we have derived two equations to describe the absorbance variation due to AuNP during the reaction (Abs_t), both when the concentration of Au(III) is higher (Eq. 5), or lower (Eq. 6) than the tyramine concentration (see supplementary material Appendix S1).

$$Abs_t = \varepsilon_{AuNP}[AuNP]_t$$
$$= \varepsilon_{AuNP,n} \frac{k_1}{k_{2,n}} \left(\frac{1 - e^{-C_{Au,0}\left(k_1 + \frac{2}{3}k_{2,n}C_{tyramine,0}\right)t}}{e^{-C_{Au,0}\left(k_1 + \frac{2}{3}k_{2,n}C_{tyramine,0}\right)t} + \frac{3k_1}{2k_{2,n}C_{Tyr,0}}} \right) \tag{5}$$

$$Abs_t = \varepsilon_{AuNP}[AuNP]_t$$
$$= \varepsilon_{AuNP,n} \frac{k_1}{k_{2,n}} \left(\frac{1 - e^{-C_{tyramine,0}\left(k_1 + k_{2,n}C_{Au,0}\right)t}}{e^{-C_{tyramine,0}\left(k_1 + k_{2,n}C_{Au,0}\right)t} + \frac{k_1}{k_{2,n}C_{Au,0}}} \right) \tag{6}$$

where

$$k_{2,n} = \frac{k_2}{n} \tag{7}$$

$$\varepsilon_{AuNP,n} = \frac{\varepsilon_{AuNP}}{n} \tag{8}$$

In these equations, $C_{Au,0}$ and $C_{Tyr,0}$ are the total Au(III) and tyramine concentrations used, n the number of Au atoms per AuNP and ε_{AuNP} the molar absorptivity of the AuNPs. Moreover, the stoichiometry of the overall reaction has also been taken into account.

$$2\ Au(III) + 3\ Tyramine \Leftrightarrow 2\ Au^0 + 3\ Tyramine_{ox} \tag{9}$$
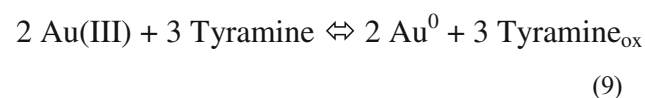
During the optimization study, the Abs = f(t) recorders obtained were fitted to the corresponding equation (Eq. 6 or Eq. 7) using Solver® and the $k_{2,n}$, k_1 y $\varepsilon_{AuNP,n}$ were obtained.

As has been indicated above (Fig. 1b), a later increase in the absorbance at the end of the process was observed, especially when the Au(III) concentration was in excess. This is usually explained by a further evolution of the formed nanoparticles, which is normally due to one of the following processes [24, 25]: a) Ostwald ripening, according to which smaller nanoparticles formed at the end of the process become dissolved to increase the size of the larger nanoparticles; or b)

Oriented attachment, referring to the coalescence of smaller nanoparticles to give larger ones. While we have no direct experimental evidence of either of these processes, it seems clear that a further reorganization of the AuNP is also produced during the enzymatic reaction. We have applied both models but neither of them properly fitted our results, so no further discussion on this part of the curve is given in this paper (see Figure S5).

Optimization of the analytical method

Although Au(III) is able to replace O_2 in the reaction, the enzyme is more prone to react with O_2 than with Au(III). This is observed when Au(III) is added at different times (incubation time) from the beginning of the reaction (see Fig. 2). As can be seen, the longer the delayed time (up to 5 min), the faster the reaction, which indicates that, when Au(III) is added, the lower the O_2 concentration in the solution, the faster the reaction. However, for 8 min incubation time the reaction becomes slower, which can be explained considering that the O_2 has diffused back from the environment surrounding the cuvette. The calculated kinetic constants k_1 and $k_{2,n}$ (table S1) show that the O_2 mainly affect the AuNP growth. Five minutes was chosen as the optimum incubation time.

Since this type of method has not been previously reported, it was considered necessary to study the effect of experimental variables on the AuNP formation. In the framework of the AuNP formation during the reaction, the following results were considered of interest: A) maximum wavelength (λmax) and bandwidth ($\Delta\lambda$, taken as the width at half of the maximum) of the plasmon band, as a measurement of the AuNP size [26, 27]; B) maximum absorbance (Abs$_{max}$) (also the $\varepsilon_{AuNP,n}$ at λ_{max}) before ripening, as a measurement of the analytical method sensitivity; and C) kinetic of the reaction (represented by the K_{Av}, k_1 and $k_{2,n}$ values).

The most critical parameter affecting the AuNP formation during the enzymatic reaction are the Au(III), TAO and

tyramine (the analyte) concentrations. Tables S2-S4 compile the Abs$_{max}$, λ_{max}, $\Delta\lambda$, k_1, $k_{2,n}$, $\varepsilon_{AuNP,n}$ and K_{Av} values obtained during the optimization studies of these parameters. The following conclusions can be derived from these studies:

1) By increasing the concentration of TAO (Fig. 3), the polydispersity of the AuNPs increase and as a consequence, the $\Delta\lambda$.

2) λmax depends on the TAO (Fig. 3) and tyramine concentrations, but in opposite senses. Although new assays are necessary to properly explain these results, a first hypothesis can be made. It is accepted that the longer the wavelength the higher the AuNP diameter [28, 29]. However, the TEM images (Fig. S1) indicated that the AuNP diameter does not appreciably change with the enzyme concentration. Thus, the λmax displacement can be attributed to the interaction between the AuNP and the protein, which according to the bibliography produces a red shift of the plasmon band [30]. Regarding the tyramine effect, probably the tyramine product of the reaction can take part of the outer sphere of the AuNP, so the spectra wavelength will be affected.

3) The overall kinetic of the reaction (see K_{Av} value) is favored, as expected, by medium-high TAO and tyramine concentrations, but the effect of both parameters on k_1 and $k_{2,n}$ is different. While TAO stimulates the growth step, tyramine increases the nucleation step. The effect of the Au(III) is of interest: K_{Av} is nearly constant up to an Au(III) concentration close to the O_2 saturation concentration ($O_{2,sat}$) in water, but higher Au(III) values produce a decrease in the overall kinetic reaction. Similarly, k_1 gives a maximum at $O_{2,sat}$ then decreases, but $k_{2,n}$ decreases monotonically with the Au(III) concentration. These results seems to indicate that Au(III) is of course necessary for AuNP formation, but it can act as an inhibitor of the enzymatic reaction.
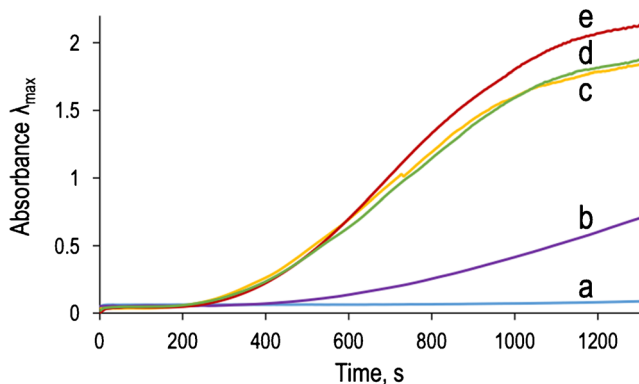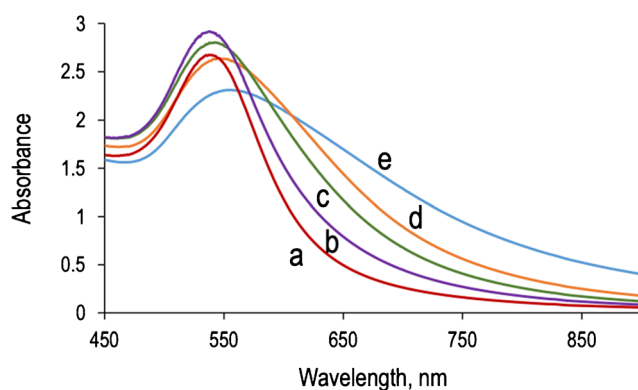
Fig. 2 Effect of the incubation time on the kinetic of the AuNP formation a) 0 min; b) 1 min; c) 3 min; d) 5 min; e) 8 min. Experimental conditions: [TAO] = 0.5 U.mL^{-1}, [Au(III)] = 1 mM, [tyramine] = 2.6×10^{-4} M and pH 7.0 phosphate buffer 0.1 M, at room temperature

Fig. 3 Effect of the TAO concentration on the absorption spectra of the formed AuNP a) 0.2 U.mL^{-1}; b) 0.5 U.mL^{-1} c) 1.0 U.mL^{-1}; d) 2 U.mL^{-1}; e) 4 U.mL^{-1}. Experimental conditions: [Au(III)] = 1 mM, [tyramine] = 2.6×10^{-4} M, incubation time 5 min and pH 7.0 phosphate buffer 0.1 M, at room temperature

4) The effect of Au(III) and TAO on the Abs_{max} is also indicated in Tables S2 and S3, and can be explained considering the variations observed in the corresponding $\varepsilon_{AuNP,n}$. The Mie theory predicts a relationship between this parameter and the cubed AuNP diameter raised to the cube (d^3) [31]. This relationship has been experimentally observed [31, 32]; an average relation is given by (see Appendix S2):

$$\varepsilon_{AuNP} = 9.2(\pm 4.1)\mathrm{x}10^4\, d^3 \quad (d, in\; nm) \quad (10)$$

If it is considered that AuNPs are spherical in shape, it is possible to relate d with the number of Au atoms present in each AuNP according to the following equation [33]:

$$n = 30.9\, d^3 \quad (d, in\; nm) \quad (11)$$

By combining Eqs. (10) and (11) the expected $\varepsilon_{AuNP,n}$ value can be obtained:

$$\varepsilon_{AuNP,n} = \frac{\varepsilon_{AuNP}}{n} = 3.0(\pm 1.3)\mathrm{x}10^3 \quad (12)$$

The values given in tables S2-S4 qualitatively (i.e., order of magnitude) agree with (Eq. 12), which validates the model given by Eqs. (5) and (6); the differences observed between the theoretical value given in Eq. 12 and those obtained experimentally can be explained considering that the AuNP are not fully spherical (Fig. S1). Moreover, Eq. (10) states that changes in the observed $\varepsilon_{AuNP,\,n}$ may be due to small variations in the d of the formed AuNP.

In order to obtain a suitable balance between kinetics, sensitivity and linear range, the Au(III) and TAO concentrations chosen were 10^{-3} M and 0.5 U.mL^{-1} respectively.

The pH effect on the TAO enzymatic reaction was studied (figure S6A) and the results were compared with those obtained by measurement of the O_2 consumption in the absence of Au(III) (figure S6B). As can be seen, the enzymatic reaction can be carried out quantitatively in a pH range from 6 to 10 in the absence of Au(III), with optimum reaction rates at pH 7.0 and 8.0. When Au(III) is used, the effect of the pH is more critical. First, the AuNP formation is observed in a narrower pH range, from 7.0–9.0; second, the Abs_{max} and the kinetic constants of the reaction depend on the pH, with an optimum at pH 7.0; third, the λ_{max} and $\Delta\lambda$ show same dependence on the pH, but 7.0 and 8.0 give similar results.

The AuNP formation is slower than the classical indicating colorimetric reactions based on HRP and a dye. To improve the kinetic of the reaction, the effect of temperature was also studied (Fig. 4). As expected, the time necessary to reach the plateau is reduced by increasing the temperature. At a
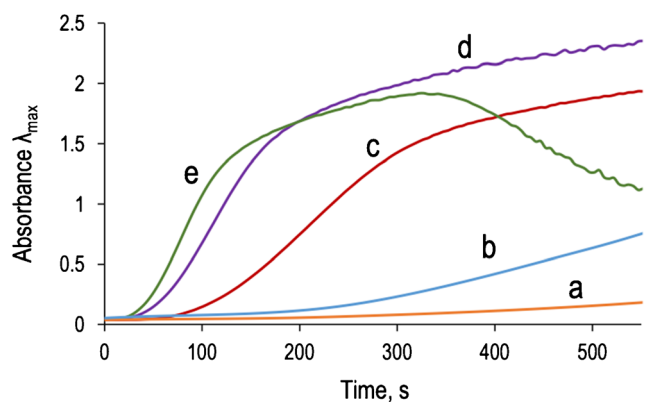

Fig. 4 Effect of the temperature on the kinetic of the reaction a) 20 °C; b) 30 °C; c) 40 °C; d) 50 °C; e) 60 °C. Experimental conditions: [TAO] = 0.5 U.mL^{-1}, [Au(III)] = 1 mM, [tyramine] = 7.9×10^{-4} M, incubation time 5 min 3and pH 7.0 phosphate buffer 0.1 M

temperature of 60 °C, after the fast increase in the absorbance a later decrease is observed due to the enzyme denaturation which destabilizes the AuNP formed. The three kinetic constants (k_1, $k_{2,n}$ and K_{Av}) increase with the temperature following the Arrhenius equation (Table S5), but its effect on the Abs_{max}, λ_{max} and $\Delta\lambda$ is negligible.

Finally, to try to improve the synthesis process of the nanoparticles during the enzymatic reaction, SiO_2 nanoparticles were added. This was intended to generate nuclei from which the gold nanoparticles grow. However, no modifications of the kinetic were observed (Figure S7).

Analytical figures of merit

The optimum experimental conditions for tyramine determination derived from the studies described above are compiled in Table 1. The experimental linear response range (Figure S8), the detection (LOD) and quantification limit (LOQ) and the RSD obtained are also compiled, working at room temperature (rt) and at 40 °C degrees. It is important to indicate that the detection limit of this method is consistent with that obtained using the classical HRP/colorant reaction.

Table 1 Analytical figures of merit obtained working at room temperature (20 °C) and 40 °C

	20 °C (rt)	40 °C
Linear range, μM	25–330	25–330
LOQ, μM	9.5	11.5
LOD, μM	2.9	3.4
RSD, % (250 μM)[a]	5.6 ($n = 5$)	6.0 ($n = 5$)

[a] The RSD obtained for all points of the calibration line linearly decrease from 11.3% (rt) or 11.8% (40 °C) obtained for 25 μM to 3.2% (rt) or 4.0% (40 °C) obtained using 330 μM

Interferences

Other amines have been studied as possible interferences in the method. To this end, putrescine, cadaverine and histamine, the main biogenic amines appearing with tyramine in real samples, were studied. Our experimental studies have shown that these three biogenic amines were not able to generate AuNP during the enzymatic reaction (at least up to 10^{-4} M). However, they affect the AuNP formation during the tyramine /TAO reaction.

First, figure S9A show the $Abs_{540nm} = f(t)$ representations obtained for tyramine in the presence of putrescine and cadaverine. As can be seen, both amines decrease the rate of the AuNP formation during the reaction but the final absorbance is not affected. Figure S9B shows that the kinetic of the O_2 consumption by the tyramine /TAO reaction is not affected by any of the amines, so the most plausible interference mechanism comes from the ability of Au(III) to form coordination complexes with diamines, $(Au(Put)_2)^{3+}$ and $(Au(Cad)_2)^{3+}$ being the expected stoichiometries [34]). These complexes decrease the kinetic of the Au(III) reduction. In order to correct this problem, several alternatives were examined. The easiest to use was increasing the kinetic of the reaction by heating at temperature of about 40 °C (figure S9C).

A more important problem was caused by the histamine:tyramine ratio. If this ratio is 1:1, the formation of nanoparticles is not observed. The general hypothesis is that histamine forms a complex, stronger than those of the putrescine or cadaverine with Au(III) that does not allow it to react following the mechanism described above [35]. This interference was not avoided by heating the solution or by adding a metallic species (Cu(II) or Zn(II)) able to react with histamine. To evaluate the magnitude of this interference, tests were performed with a constant concentration of tyramine and varying the amounts of histamine present in the reaction. Figure S10A shows the absorption spectra obtained. It can be observed that the decrease in the signal is proportional to the histamine presents in the sample (Figure S10B). This type of interference can be estimated by performing a doping of the sample with a known concentration of tyramine and observing how the signal decreases depending on the amount of histamine present.

Real sample

Many types of samples contain tyramine as the majority biogenic amine. An example is Emmental cheese, so we applied this method to tyramine determination in a sample of this cheese.

Using the optimized experimental conditions (and working at 40 °C), we applied the method explained in the experimental section and the standard addition method to avoid interferences of the matrix. In Figure S11 it can be seen that the slope of the line does not differ significantly from the slope of the line for which no sample is added, so no proportional interferences were observed. The concentration of tyramine in the sample obtained was 93 ± 14 mg Kg^{-1} ($n = 5$). The sample was also analyzed by the Public Health Laboratory of Aragón using their HPLC validated method (86 ± 13 mg Kg^{-1}, $n = 3$) and a colorimeter method based on TAO but using HRP/TMB as the indicating reaction (see Appendix S3). No significant differences were observed between the methods.

Conclusions

This paper has demonstrated the possibility of generating AuNP during an enzymatic reaction and using the corresponding plasmon resonance band as the analytical signal, thus avoiding, in this way, the chromogen/HRP indicating reaction. Although several theoretical aspects need more in-depth studies, the results suggest that this is a general mechanism which can work with many other enzymatic reactions. Moreover, other types of analytical signals deserve to be studied, such as: the fluorescence of gold nanoclusters, which is expected to appear during the nucleation process, and/or the surface-enhanced Raman signal of the enzyme or the reaction product, as a consequence of the AuNP formation. Finally, this method may also be carried out using other types of metallic species able to generate nanoparticles (especially, Ag(I)).

Compliance with ethical standards

Conflict of interest The author(s) declare that they have no competing interests.

References

1. Benkerroum N (2016) Biogenic amines in dairy products: origin, incidence, and control means. Compr Rev Food Sci Food Saf 15: 801–826. https://doi.org/10.1111/1541-4337.12212

2. Karovičová J, Kohajdová Z (2005) Biogenic amines in food. Chem Pap 59:70–79

3. Papageorgiou M, Lambropoulou D, Morrison C, Kłodzińska E, Namieśnik J, Płotka-Wasylka J (2018) Literature update of analytical methods for biogenic amines determination in food and beverages. Trac-Trend Anal Chem 98:128–142. https://doi.org/10.1016/j.trac.2017.11.001

4. Ordóñez JL, Troncoso AM, García-Parrilla MDC, Callejón RM (2016) Recent trends in the determination of biogenic amines in fermented beverages–a review. Anal Chim Acta 939:10–25. https://doi.org/10.1016/j.aca.2016.07.045

5. Wouters J, Perpete P, Hayen P, Anceau N, Durant F (1994) Kinetic characterization of tyramine oxidase of Arthrobacter species. Biochem Mol Biol Int 32:737–743

6. Lata S, Yadav S, Bhardwaj R, Pundir CS (2011) Amperometric determination of tyramine in sauce and beer by epoxy resin biocomposite membrane bound tyramine oxidase. Sens Instrum Food Qual Saf 5:104–110. https://doi.org/10.1007/s11694-011-9117-5

7. Lange J, Wittmann C (2002) Enzyme sensor array for the determination of biogenic amines in food samples. Anal Bioanal Chem 372:276–283. https://doi.org/10.1007/s00216-001-1130-9

8. Osman AM, Wong KKY, Fernyhough A (2006) ABTS radical-driven oxidation of polyphenols: isolation and structural elucidation of covalent adducts. Biochem Biophys Res Commun 346:321–329. https://doi.org/10.1016/j.bbrc.2006.05.118

9. Scott SL, Chen WJ, Bakac A, Espenson JH (1993) Spectroscopic parameters, electrode potentials, acid ionization constants, and electron exchange rates of the 2, 2′-azinobis (3-ethylbenzothiazoline-6-sulfonate) radicals and ions. J Phys Chem 97:6710–6714. https://doi.org/10.1021/j100127a022

10. Zamborini FP, Bao L, Dasari R (2011) Nanoparticles in measurement science. Anal Chem 84:541–576. https://doi.org/10.1021/ac203233q

11. Sabela M, Balme S, Bechelany M, Janot JM, Bisetty K (2017) A review of gold and silver nanoparticle-based colorimetric sensing assays. Adv Eng Mater 9:1700270. https://doi.org/10.1002/adem.201700270

12. Liu BW, Wu YY, Huang PC, Wu FY (2019) Colorimetric determination of cytosine-rich ssDNA by silver (I)-modulated glucose oxidase-catalyzed growth of gold nanoparticles. Microchim Acta 186:467–468. https://doi.org/10.1007/s00604-019-3591-6

13. Li G, Yang M, Chen LC, Gao B, Xiong XL (2015) Colorimetric and visual detection of tyrosine based on its copper-catalyzed enzymatic oxidation to dopamine and subsequent reductive formation of colored gold nanoparticles using copper ions. Microchim Acta 182:13–117. https://doi.org/10.1007/s00604-014-1278-6

14. López-Lorente AI, Valcárcel M (2016) The third way in analytical nanoscience and nanotechnology: involvement of nanotools and nanoanalytes in the same analytical process. Trac-Trend Anal Chem 75:1–9. https://doi.org/10.1016/j.trac.2015.06.011

15. Xie J, Zheng Y, Ying JY (2009) Protein-directed synthesis of highly fluorescent gold nanoclusters. J Am Chem Soc 131:888–889. https://doi.org/10.1021/ja806804u

16. Newman JDS, Blanchard GJ (2006) Formation of gold nanoparticles using amine reducing agents. Langmuir 22:5882–5887. https://doi.org/10.1021/la060045z

17. Bai J, Flowers K, Benegal S, Calizo M, Patel V, Bishnoi SW (2009) Using the enzymatic growth of nanoparticles to create a biosensor. An undergraduate quantitative analysis experiment. J Chem Educ 86:712. https://doi.org/10.1021/ed086p712

18. Alonso-de Castro S, Cortajarena AL, López-Gallego F, Salassa L (2018) Bioorthogonal catalytic activation of platinum and ruthenium anticancer complexes by FAD and flavoproteins. Angew Chem Int Ed 130:3197–3201. https://doi.org/10.1002/ange.201800288

19. Quist DA, Diaz DE, Liu JJ, Karlin KD (2017) Activation of dioxygen by copper metalloproteins and insights from model complexes. J Biol Inorg Chem 22:253–288. https://doi.org/10.1007/s00775-016-1415-2

20. Thanh NT, Maclean N, Mahiddine S (2014) Mechanisms of nucleation and growth of nanoparticles in solution. Chem Rev 114:7610–7630. https://doi.org/10.1021/cr400544s

21. You H, Fang J (2016) Particle-mediated nucleation and growth of solution-synthesized metal nanocrystals: a new story beyond the LaMer curve. Nano Today 11:145–167. https://doi.org/10.1016/j.nantod.2016.04.003

22. Watzky MA, Finke RG (1997) Transition metal nanocluster formation kinetic and mechanistic studies. A new mechanism when hydrogen is the reductant: slow, continuous nucleation and fast autocatalytic surface growth. J Am Chem Soc 119:10382–10400. https://doi.org/10.1021/ja9705102

23. Finney EE, Finke RG (2008) Nanocluster nucleation and growth kinetic and mechanistic studies: a review emphasizing transition-metal nanoclusters. J Colloid Interface Sci 317:351–374. https://doi.org/10.1016/j.jcis.2007.05.092

24. Brazeau AL, Jones ND (2009) Growth mechanisms in nanocrystalline lead sulfide by stopped-flow kinetic analysis. J Phys Chem C 113:20246–20251. https://doi.org/10.1021/jp907270x

25. Shields SP, Richards VN, Buhro WE (2010) Nucleation control of size and dispersity in aggregative nanoparticle growth. A study of the coarsening kinetics of thiolate-capped gold nanocrystals. Chem Mater 22:3212–3225. https://doi.org/10.1021/cm100458b

26. Burda C, Chen X, Narayanan R, El-Sayed MA (2005) Chemistry and properties of nanocrystals of different shapes. Chem Rev 105:1025–1102. https://doi.org/10.1021/cr030063a

27. Enoch S, Quidant R, Badenes G (2004) Optical sensing based on plasmon coupling in nanoparticle arrays. Opt Express 12:3422–3427. https://doi.org/10.1364/OPEX.12.003422

28. Haiss W, Thanh NT, Aveyard J, Fernig DG (2007) Determination of size and concentration of gold nanoparticles from UV− Vis spectra. Anal Chem 79:4215–4221. https://doi.org/10.1021/ac0702084

29. Khlebtsov NG (2008) Determination of size and concentration of gold nanoparticles from extinction spectra. Anal Chem 80:6620–6625. https://doi.org/10.1021/ac800834n

30. Shi X, Li D, Xie J, Wang S, Wu Z, Chen H (2012) Spectroscopic investigation of the interactions between gold nanoparticles and bovine serum albumin. Chin Sci Bull 57:1109–1115. https://doi.org/10.1007/s11434-011-4741-3

31. Liu X, Atwater M, Wang J, Huo Q (2007) Extinction coefficient of gold nanoparticles with different sizes and different capping ligands. Colloid Surface B 58:3–7. https://doi.org/10.1016/j.colsurfb.2006.08.005

32. Jain PK, Lee KS, El-Sayed IH, El-Sayed MA (2006) Calculated absorption and scattering properties of gold nanoparticles of different size, shape, and composition: applications in biological imaging and biomedicine. J Phys Chem B 110:7238–7248. https://doi.org/10.1021/jp057170o

33. Leff DV, Ohara PC, Heath JR, Gelbart WM (1995) Thermodynamic control of gold nanocrystal size: experiment and theory. J Phys Chem 99:7036–7041. https://doi.org/10.1021/j100018a041

34. Mironov IV, Afanas'eva VA (2010) Gold (III) amine complexes in aqueous alkali solutions. Russ J Inorg Chem + 55:1156–1161. https://doi.org/10.1134/S0036023610070302

35. Sjöberg S (1997) Critical evaluation of stability constants of metal-imidazole and metal-histamine systems (technical report). Pure Appl Chem 69:1549–1570. https://doi.org/10.1351/pac199769071549